MATEC Web of Conferences **67**, 06106 (2016) DOI: 10.1051/matecconf/20166706106
SMAE 2016

Photo electrochemical Performance and Photo catalytic Activity of Porous WO_3 Films using Polystyrene Spheres as Templates

Guanhua Jin [a] and Suqin Liu [b]
School of Chemistry and Chemical Engineering, Central South University, Changsha 410083 China
[a]guanhuajin@foxmail.com[1], [b] suqinliu@foxmail.com

Abstract. Porous WO_3 films were successfully synthesized by a simple and easy method using polystyrene spheres (PS) as templates. The PS array covered F: SnO_2 coated glass (FTO) as the substrate was first prepared via electrodeposition method. Ordered porous WO_3 films were obtained by electrophoretic deposition in peroxy-tungstic acid sol. The characterization and photo electrochemical properties of samples were investigated. The results show that the porous WO_3 film displays the enhanced performance compared with the compact films without PS templates.

1. Introduction

Porous semiconducting films have attracted considerable attention because of their various applications in photocatalytic, electrochemical systems, including photovoltaic solar cells [1], electrochromic windows [2], electrocatalysts [3]. Compared with compact films, the porous films exhibit a large specific surface area, high porosity, and excellent photo absorption performance. Various porous films, such as TiO_2, ZnO nanoporous films were synthesized and investigated for conversion solar energy into chemical energy [1, 4]. However, the band gaps of TiO_2 and ZnO are larger than 3.0 eV, which means these materials can only show activity under UV irradiation. Besides the most investigated cases of TiO_2 and ZnO, WO_3 has been also suggested as a promising photoelectrode because it has a bandgap of 2.5–2.8 eV and good electron transport properties [5-7]. Tungsten oxide is a stable photocatalyst for water splitting. Moreover, WO_3 does undergo photocorrosion and is highly stable in aqueous solutions under acidic conditions, making it a promising photocatalytic material [8, 9].

The template method has been one of the most attractive methods used to obtain ordered porous films. Han et. al prepared 2D or 3D ordered porous ZnO films by electrodeposition method using 3D opal templates [10], Zhang et.al [11] synthesized porous Bi_2WO_6 films via spin-coating method using carbon-sphere as template. The templates usually prepared via vertical sedimentary [11, 12], dip-coating technique [13] and electrophoretic deposition [14]. However, the vertical sedimentary takes a few days to form the template and the experiment

* Corresponding author:guanhuajin@foxmail.com

must be kept in a vibrationless circumstance, and the dip-coating method usually requires repeat to form a regular multilayer. In comparison, the electrodeposition for the PS template usually takes several minutes and not very rigorous in the experimental condition. For the electrodeposition method to assemble the template is convenient and controllable.

In this paper, a simple and easy method was successfully used to synthesize porous WO_3 films using PS as templates. The PS array covered F: SnO_2 coated glass (FTO) as the substrate was first prepared via electrodeposition method. The ordered porous WO_3 films were obtained by electrophoretic deposition in tungsten oxide sol. The photoelectrochemical performances under visible light were also investigated.

2. Experimental Section

2.1Preparation of Polystyrene Sphere Templates and Porous WO3 Films

All chemicals were analytical grade. The latex spheres were prepared according to the method described in previous work [15]. WO_3 films were synthesized by electrophoretic deposition from peroxy-tungstic acid sol (Fig. 1b). The peroxy-tungstic acid sol was prepared by dissolution of 5 g of tungsten metal powder (W) in 20 mL of 30% hydrogen peroxide (H_2O_2) in the ice-water bath, which took about 6 h. The excess H_2O_2 was decomposed through platinum net. The solution was diluted to 60 mL by adding with 40 mL of 10/30 *v*/*v* glacial acetic acid (CH_3COOH) /anhydrous absolute ethanol (CH_3CH_2OH). The resulting solution was refluxed at 65 ℃ for 2 h yielded the bright yellow-colored deposition sol. A three-electrode configuration electrodeposition system was used to prepare WO_3 porous films at room temperature under a constant E_{dep}=-0.45 V for 2 min, with an Ag/AgCl (KCl saturated), Pt foil and the PS array-coated FTO as the reference electrode, anode electrode and working electrode, respectively. The resulted films were immediately rinsed with deionized water and dried in air. The synthesized films were calcined in air at 450℃ for 3 h with the heating rate of 1℃/min.

2.2Characterization and Photoelectrochemical Measurements

The structures and phases of the film samples were determined via X-ray diffraction (XRD) using a Rigaku D/MAX PC2200 diffractometer operating with a Cu Kα radiation at a scan rate of 0.02°•s-1. The accelerated voltage and applied current were 40 kV and 40 mA, respectively. The morphology of WO_3 was observed using a JSM-6700F field emission scanning electron microscope (FESEM) (JEOL, Japan) at an acceleration voltage of 20 kV. The chemical compositions of the films were identified by X-ray photoelectron spectroscopy (XPS, K-Alpha 1063, Thermo Fisher Scientific) employing monochromatic Al Kα excitation. The spectra were calibrated according to the binding energy of the C1s peak at 284.8 eV and the spectral processing was conducted with the Thermo Avantage software. UV–vis spectras were obtained with a Shimadzu 2450 spectrophotometer in the scanning range of 300–700 nm wavelength.

The photoelectrochemical properties of the samples were determined using an electrochemical workstation (Zennium, Zahner, Germany). A three-electrode system consisting of a Pt foil as the counter electrode, Ag/AgCl(KCl saturated)as the reference electrode, and the treated WO_3 porous film sample as the working electrode was constructed in an aqueous 0.5 M H_2SO4 electrolyte via irradiation. The illumination source was a 150 W

xenon lamp with a 400 nm cutoff filter to remove UV irradiation. Incident-photon-to-current-efficiencies (IPCE) measurements were carried out using a xenon lamp (150 W, Oriel) with an AM 1.5 filter and a monochromator with a bandwidth of 5 nm.

3. Results and Discussion

3.1SEM and XRD

Fig.1a shows the scanning electron microscopy (SEM) images of the ordered structure of PS sphere array. The PS spheres with diameter of about 260 nm were piled up to two or more layers on the substrate and stacked in a face-centered cubic structure. The (111) plane of the electrodeposition colloidal crystal is parallel to the FTO substrate. With a 2 min electrophoretic deposition on the PS template substrate, the ordered porous films calcined in air at 450℃ for 3 h could be obtained. However, only compact films formed through the same electrophoretic deposition processing on the FTO substrate without PS sphere array. The average of diameter of pore is 250 nm, which is agreement with the diameter of the PS sphere. The inset of the Fig. 2b shows the fracture surface of the porous WO_3 films. The film has a uniform thickness of 520 nm and it is obvious that the film is about two layers thick of the PS sphere.

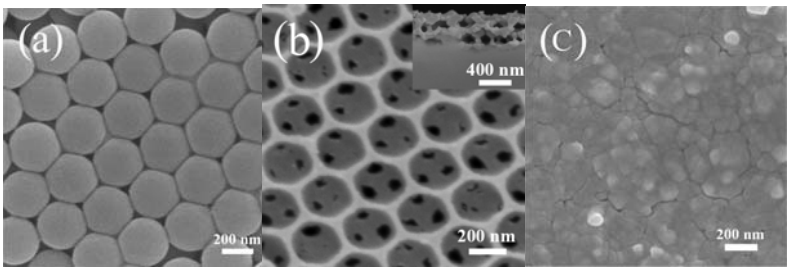

Fig. 1 The SEM images of (a) the PS spheres template (b) porous WO_3 film (c) compact WO_3 film

Fig. 2 shows the X-ray diffraction (XRD) patterns of porous and compact WO_3 films. The peaks of WO_3 could be well assigned and the signals from FTO substrate and WO_3 were also detected. Both compact and porous WO_3 films are monoclinic for three peaks at 2θ = 22°–25° corresponding to the (002), (020) and (200) lattice planes of monoclinic WO_3 (JPCDS 83-0950). No additional peaks were detected at the sensitivity limit of the instrument, suggesting that the inverted porous assembly with PS colloidal crystal template did not affect the intrinsic crystallization characteristic of WO_3 derived from the electrophoretic deposition processing. The particle size can be obtained from the Scherrer Equation by using the (002) diffraction peak [16]. The size of the compact WO_3 crystallites is 37.3 nm while the porous WO_3 is 37.9 nm. Both the two films get the full grow and with the same crystallinity under the same calcination temperature, the crystallinity does not be affected by the PS crystal template. Moreover, the intensity of (002), (020) and (200) peak of porous film is weaker that of the compact film, which is attributed to the X-ray scattering resulted by the porous structure.

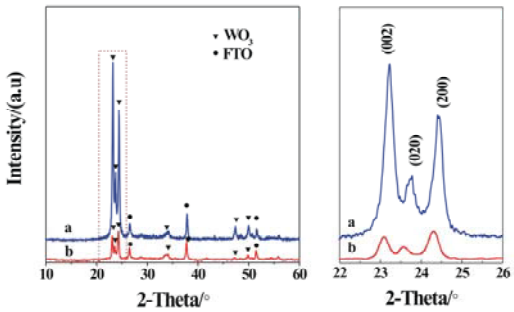

Fig. 2 The XRD patterns of (a) compact WO_3 film and (b) porous WO_3 film

3.2XPS Studies

XPS measurement was carried to elucidate the surface chemical composition and C1s core level of the porous WO_3 film. The binding energies for W4f7/2 and Wf5/2 peak were observed at 35.48 and 37.48 eV for the sample (Fig. 3b), and for O 1s at 530.28 eV (Fig. 3c), which is in a good agreement with the literature for WO_3 [6]. In the C1s spectra, binding energies of 284.59 eV and 286.93 eV were observed for the compact WO_3 sample (Fig. 3d), while binding energies of 284.72 eV and 285.98 eV were observed for the porous sample (Fig. 3e). These peaks were detected for both samples due to the presence of the carbon-containing contamination onto samples' surfaces caused by pumping, which is an unavoidable presence on all air exposed materials. The peak at 288.18 eV corresponded to a carbonate species, which might be attributed to the C=O group. These results are in agreement with the studies reported by Ding [17] and Sun[18] , suggesting that the carbon was doped into the lattice of the WO_3 phase during the calcination process.

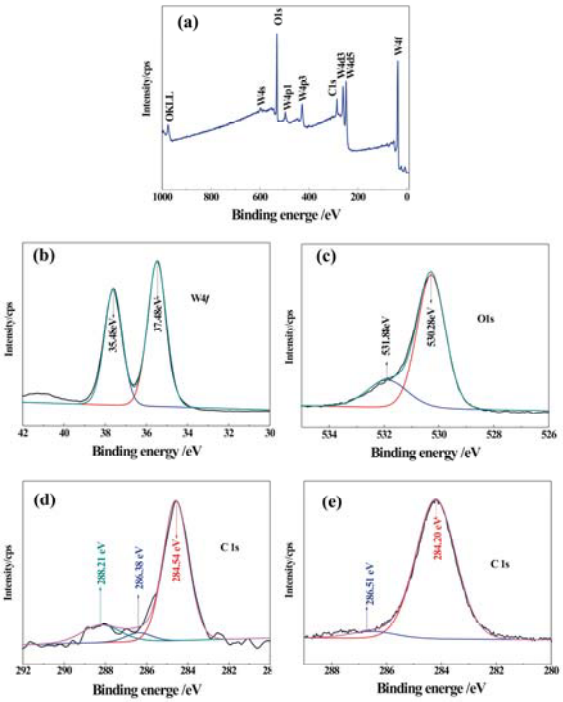

Fig. 3 The XPS patterns of WO_3 films: (a) the full spectrum of porous WO_3 film, (b) W4f region, (c) O 1s region and (d) C 1s regions of porous WO_3 film, (e) the C1s regions of compact WO_3 film

3.3UV-vis Spectroscopy

The UV–vis transmission spectra of the compact and porous WO_3 films are shown in Fig. 4. Compared to the compact sample, the porous WO_3 absorptions are higher in both ultraviolet and visible region. The increased absorbance of porous WO_3 film can be attributed to the porous surface. Incident photons are more effectively absorbed on the porous electrode than on the flat electrode because of light scattering within the porous structure [19]. The scattering efficiency of the porous structure expands the opal path length, which could lead to the improvement of the light absorption efficiency [20]. The absorption edge of porous film falls into the visible region at the wavelength of 400 nm.

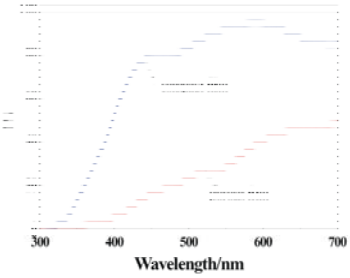

Fig. 4 The UV-vis transmission spectrums compact and porous WO_3 films

3.4Photoelectrochemical Performances

The photochemical performances of both compact and porous films were investigated. Fig. 5 shows the photocurrent-voltage curves of porous and compact WO_3 films. It is obvious that an enhanced photocurrent was obtained. Particularly, the photocurrent density at 1.2 V vs. Ag/AgCl of the porous film calcined at 450℃ is 1.61 $mA \cdot cm^{-2}$, which was almost two times as high as that of the compact film (0.76 $mA \cdot cm^{-2}$). The porous structure has the higher exposed surface area with the electrolyte; a larger part of the structure is affected by the field of the Schottky junction at the semiconductor electrolyte interface. The efficiency of charge-carrier transportation was higher in the WO_3 porous film than in the compact film.

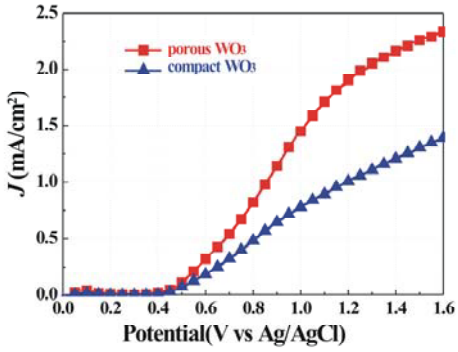

Fig. 5 Linear sweep voltammogram curves of the porous and compact WO_3 films in 0.5 $mol \cdot L^{-1}$ H_2SO_4 solution from 0~1.6 V.

4. Conclusion

In summary, a uniform and highly oriented assembly of WO_3 porous film with a diameter of 250 nm onto FTO coated glass by means of an electrophoretic deposition process using polystyrene spheres as templates. The porous films adopt a monoclinic structure after annealing. The annealed WO_3 porous films exhibit high photochemical performance because of their porous structure offering more reaction sites. Our findings provide an approach to fabricate transparent metal oxide films with porous structures for optical applications.

5. Acknowledgments

This study was supported by the Fundamental Research Funds for the Central Universities of Central South University (grants no. 2014zzts016)

References

1. A. Tricoli, A.S. Wallerand, M. Righettoni, Highly porous TiO_2 films for dye sensitized solar cells, J. Mater. Chem.. 22 (2012) 14254-14261.
2. B. Baloukas, J.-M. Lamarre, L. Martinu,Electrochromic interference filters fabricated from dense and porous tungsten oxide films, Sol. Energ. Mat. Sol. C.. 95 (2011) 807-815.
3. Y. Yang, H. Fei, G. Ruan, C. Xiang, J.M. Tour,Efficient electrocatalytic oxygen evolution on amorphous nickel–cobalt binary oxide nanoporous layers, ACS nano. 8 (2014) 9518-9523.
4. B. Pal, M. Sharon,Enhanced photocatalytic activity of highly porous zno thin films prepared by sol–gel process, Mater. Chem. Phys.. 76 (2002) 82-87.
5. C.G. Granqvist, Handbook of inorganic electrochromic materials, Elsevier Science Ltd, 1995.
6. W. Li, J. Li, X. Wang, S. Luo, J. Xiao, Q. Chen, Visible light photoelectrochemical responsiveness of self-organized nanoporous WO_3 films, Electrochim. Acta. 56 (2010) 620-625.
7. J. Yang, W. Li, J. Li, D. Sun, Q. Chen,Hydrothermal synthesis and photoelectrochemical properties of vertically aligned tungsten trioxide (hydrate) plate-like arrays fabricated directly on fto substrates, J. Mater. Chem. 22 (2012) 17744-17752.
8. M. Butler,Photoelectrolysis and physical properties of the semiconducting electrode wo_3, J. Appl. Phys. 48 (1977) 1914-1920.
9. V. Chakrapani, J. Thangala, M.K. Sunkara,Wo_3 and w_2n nanowire arrays for photoelectrochemical hydrogen production, Int. J. Hydrogen. Energ. 34 (2009) 9050-9059.
10. H. Yan, Y. Yang, Z. Fu, B. Yang, L. Xia, S. Fu, F. Li,Fabrication of 2d and 3d ordered porous zno films using 3d opal templates by electrodeposition, Electrochem. Commun. 7 (2005) 1117-1121.
11. L.W. Zhang, Y.J. Wang, H.Y. Cheng, W.Q. Yao, Y.F. Zhu,Synthesis of porous Bi_2WO_6 thin films as efficient visible©\light©\active photocatalysts, Adv. Mater. 21 (2009) 1286-1290.
12. J. Li, S. Luan, W. Huang, Y. Han,Colloidal crystal heterostructures by a two-step vertical deposition method, Colloid Surf. A-Physicochem. Eng. Asp.. 295 (2007) 107-112.
13. Z. Liu, J. Ya, Y. Xin, J. Ma, C. Zhou,Assembly of polystyrene colloidal crystal

templates by a dip-drawing method, J. Cryst. Growth. 297 (2006) 223-227.
14. Böhmer,In situ observation of 2-dimensional clustering during electrophoretic deposition, Langmuir. 12 (1996) 5747-5750.
15. Z. Liu, Z. Jin, J. Qiu, X. Liu, W. Wu, W. Li,Preparation and characteristics of ordered porous zno films by a electrodeposition method using ps array templates, Semiconductor science and technology. 21 (2006) 60.
16. M. Saif, M.S.A. Abdel-Mottaleb,Titanium dioxide nanomaterial doped with trivalent lanthanide ions of tb, eu and sm: Preparation, characterization and potential applications, Inorg. Chim. Acta. 360 (2007) 2863-2874.
17. X. Ding, D. Zeng, S. Zhang, C. Xie,C-doped wo3 microtubes assembled by nanoparticles with ultrahigh sensitivity to toluene at low operating temperature, Sens. Actuators, B. 155 (2011) 86-92.
18. Y. Sun, C.J. Murphy, K.R. Reyes-Gil, E.A. Reyes-Garcia, J.M. Thornton, N.A. Morris, D. Raftery,Photoelectrochemical and structural characterization of carbon-doped wo3 films prepared via spray pyrolysis, Int. J. Hydrogen. Energ. 34 (2009) 8476-8484.
19. F.I. Marin, M.A. Hamstra, D. Vanmaekelbergh,Greatly enhanced sub-bandgap photocurrent in porous gap photoanodes, J. Electrochem. Soc. 143 (1996) 1137-1142.
20. U. Akira,Theoretical study of application of multiple scattering of light to a dye-sensitized nanocrystalline photoelectrichemical cell, Chem. Phys. Lett. 277 (1997) 105-108.